The Abdus Salam
International Centre for Theoretical Physics

United Nations
Educational, Scientific and
Cultural Organization

IAEA
International Atomic Energy Agency

**SMR/1849-18**

**Conference and School on Predictability of Natural Disasters for our Planet in Danger. A System View; Theory, Models, Data Analysis**

***25 June - 6 July, 2007***

# Theory of Error Growth
# Growth of Random Errors

V. Krishnamurthy

*Center for Ocean-Land-Atmosphere Studies, Calverton, USA*
*& George Mason University, Fairfax, USA*

# Theory of Error Growth

## Lecture 3
## Growth of Random Errors

**V. Krishnamurthy**

Center for Ocean-Land-Atmosphere Studies
Institute of Global Environment and Society
Calverton, MD 20705, USA
and
Department of Climate Dynamics
George Mason University
Fairfax, VA 22030, USA

Conference and School on Predictability of Natural Disasters for our Planet in Danger
A Systems View: Theory, Models and Data Analysis
The Abdus Salam International Centre for Theoretical Physics, Trieste, Italy
25 June – 6 July 2007

## Growth of an ensemble of initial errors

### Error growth in Quadratic Map

The examples of error growth in the quadratic map showed that the growth rate of the error $X_n' - X_n$ depends on the true state $X_n$. To obtain the behavior of the average error growth of the system, the evolution of a large ensemble of initial errors must be considered. The ensemble mean of the errors will provide estimates of average rate of error growth and the time taken to reach saturation.

When the initial errors are introduced at many different points in the basic solution, the ensemble average error provides the *global error growth* of the system.

When the initial errors are introduced at a single point in the basic solution, the *local error growth* is obtained.

### Local growth

Introduce 10000 initial errors at one point and study the evolution of the ensemble mean error.

### Global growth

Introduce one initial error at 10000 points and study the evolution of the ensemble mean error.

The error is expressed as the root mean square (rms) error, a commonly used measure of error. The ensemble mean error gives the average growth of error.

## Local Growth

At one particular time step in the basic solution, 10000 initial errors are introduced. The subsequent evolutions of the basic solution and the perturbed solutions are computed to obtain the time series of an ensemble of errors.

The ensemble mean error is plotted as a function of time step, starting with the initial mean error equal to 0.001.

The error growth reflects the local character with fluctuations. The error reaches saturation at about time step 20. The saturated error also shows considerable fluctuation.

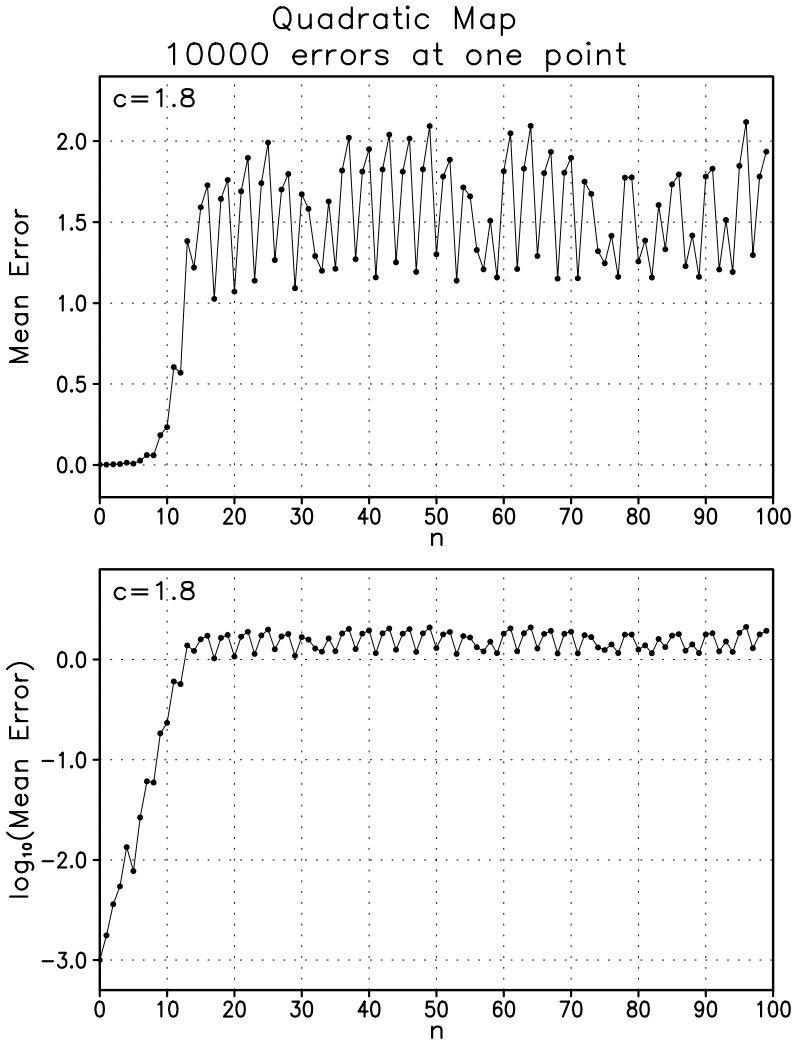

## Global Growth

At 10000 different time steps in the basic solution, an error of 0.001 is added to use as initial conditions for perturbed solutions. The subsequent evolution of the basic state and the perturbed states are computed to obtain the time series of an ensemble of errors.

The ensemble mean error is plotted as a function of time step, starting with the initial mean error equal to 0.001.

The error growth is smoother because of averaging over many local errors.
The growth is almost perfectly exponential at first with an amplification factor of about 1.5 per time step. The error nearly ceases to grow at about step 35 and reaches saturation.

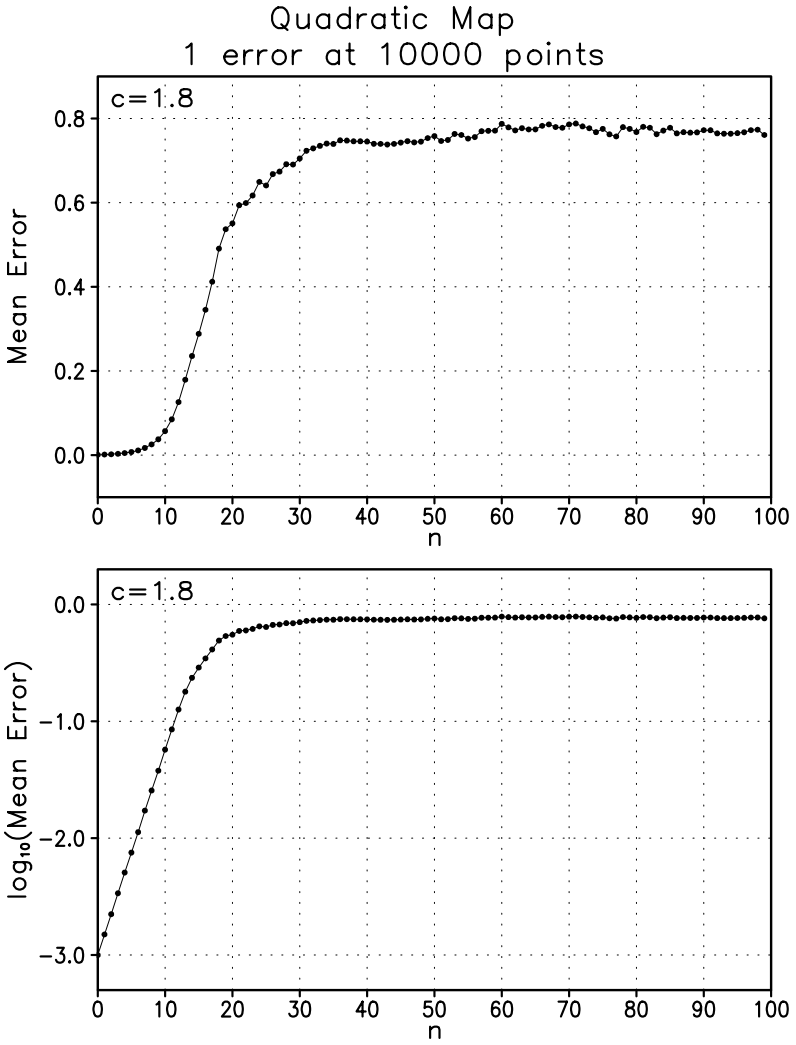

## Growth of random errors in 28-variable Lorenz model

(Krishnamurthy, V., 1993: A predictability study of Lorenz's 28-variable model as a dynamical system. *J. Atmos. Sci.*, **50**, 2215-2229**)**

### Model

The model represents a two-layer quasi-geostrophic mid-latitude atmosphere forced by Newtonian heating with dissipation occurring through frictional drags at the surfaces. The model is transformed into spectral form by expanding the dependent variables in a set of orthonormal functions. The low-order spectral truncation results in a 28-variable model (i.e., 28 ordinary differential equations).

This model's attractors are chaotic for a range of values of the forcing (heating) parameter.

The error growth will be discussed for the chaotic attractor at $\theta_0^*$=0.1.

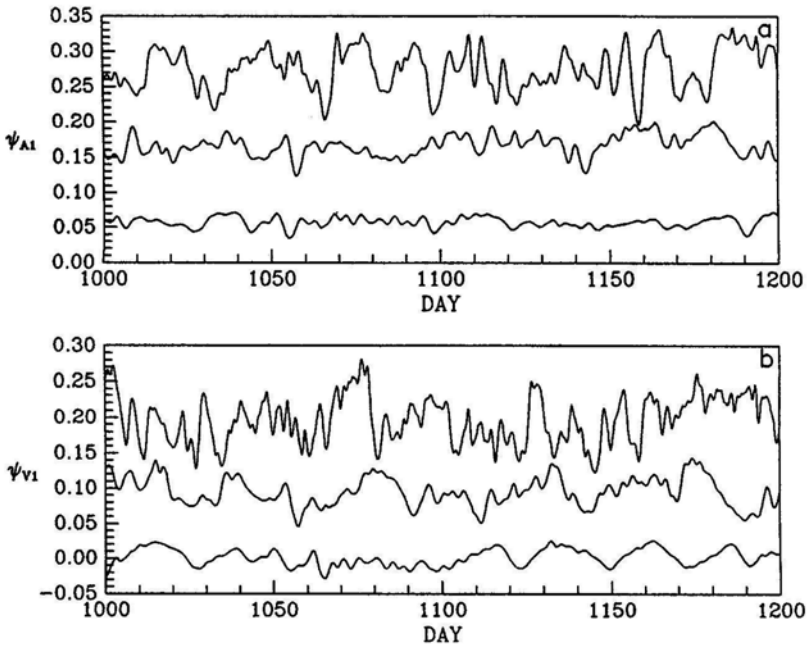


FIG. 1. Time series of (a) zonal component $\psi_{A1}$ and (b) wave component $\psi_{V1}$ of the streamfunction for $\theta_0^* = 0.08$ (lower curve), 0.1 (middle curve), and 0.15 (upper curves); $\psi_{A1}$ and $\psi_{V1}$ are the coefficients of the largest scale functions $\Phi_1$ and $\Phi'_{11}$, respectively, in the spectral expansion of the streamfunction. The scales of $y$ axes apply to $\theta_0^* = 0.08$; the curves for $\theta_0^* = 0.1$ and 0.15 have been displaced upward by 0.1 and 0.2 units, respectively, for clarity.

## 28-variable Lorenz model: Local growth of individual errors

Five different random errors are introduced at one point in the attractor (left) and errors are introduced at five different points in the attractor (right). The errors grow exponentially for a while and slow down before reaching saturation.

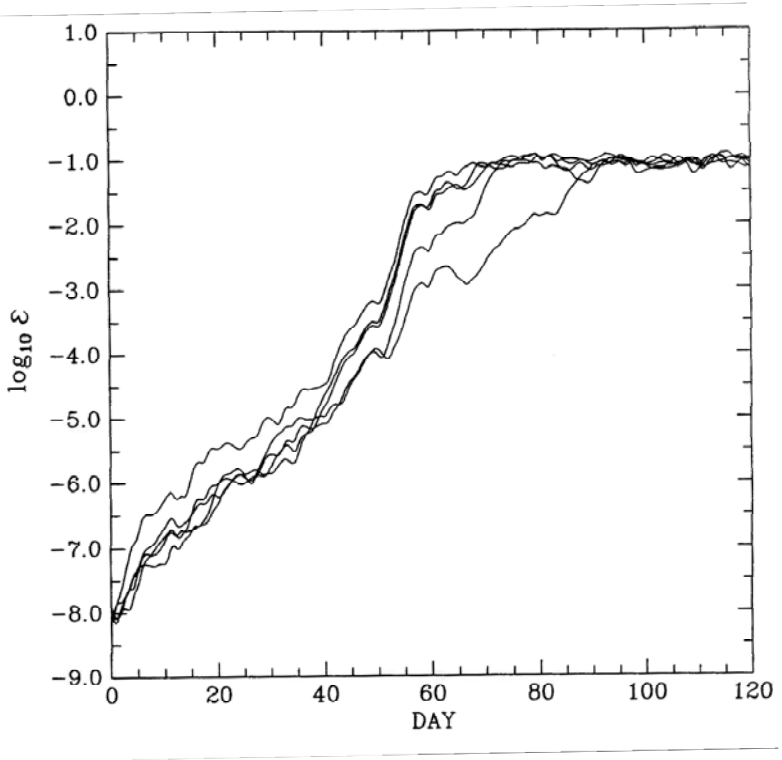


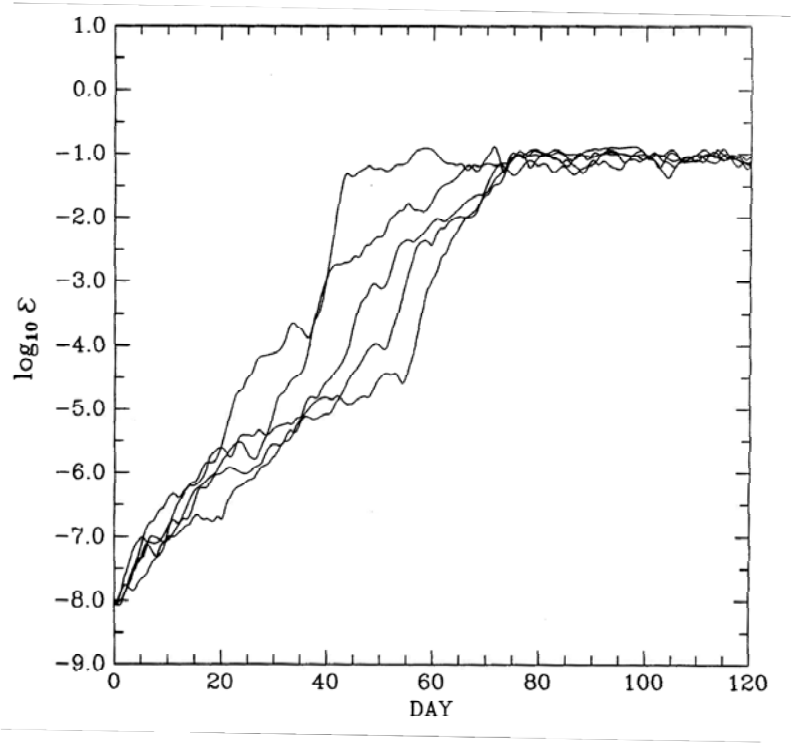

## 28-variable Lorenz model: Ensemble-averaged local growth

Four ensembles, each with 500 initial random errors, were allowed to evolve from a particular state in the attractor. The initial size of the ensemble mean error is different. It takes about 10 days for the error with the largest initial size to reach saturation while it takes about 70 days for the error with the smallest initial size.

All four error curves show parallel growth indicating the local nature of the error growth.

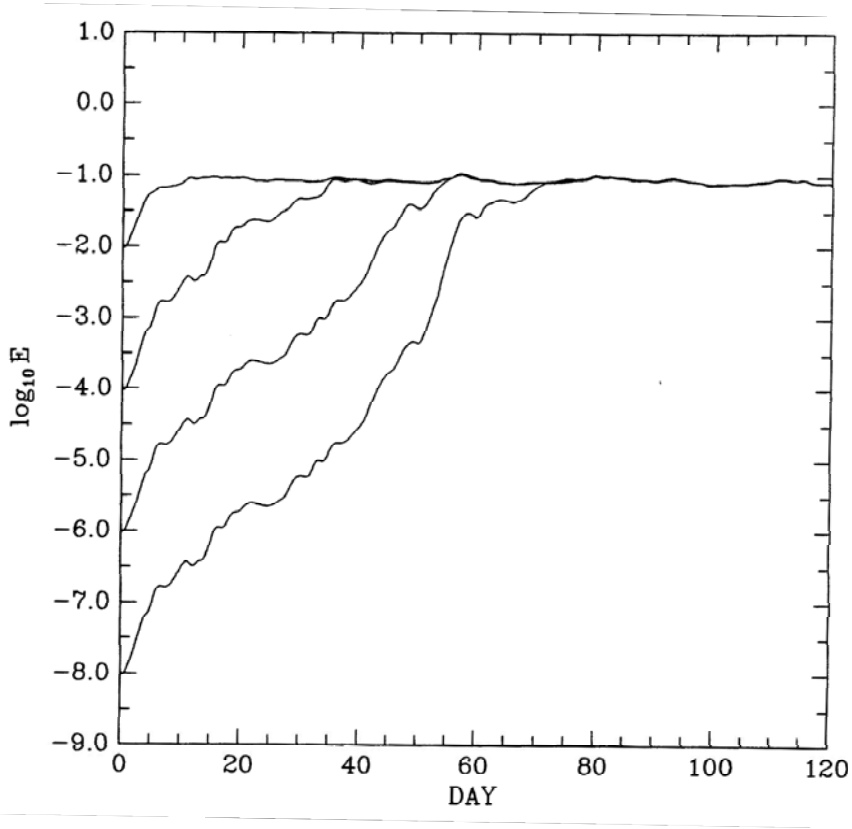

## 28-variable Lorenz model: Global growth of errors

Ensemble mean of growth of random errors introduced at 1000 different states in the attractor shows smooth growth. The geometric mean error (solid) is smoother than the arithmetic mean error (dashed). The growth is exponential during much of the growth phase before saturation.

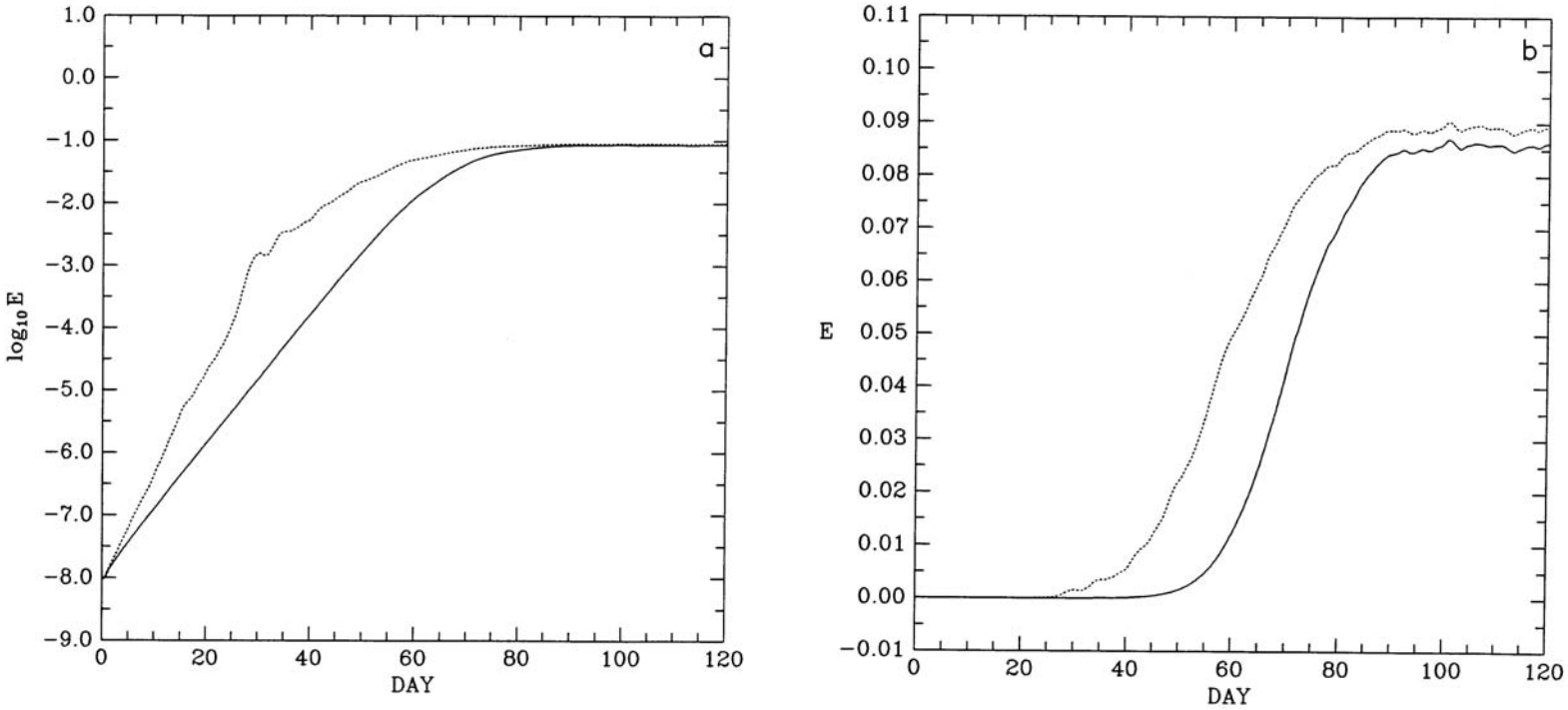

The geometric mean of random errors (dashed) is shown along with exponential growth according the first four Lyapunov exponents i.e., $(a)\ \exp(\lambda_1 t)$, $(b)\ \exp(\lambda_2 t)$, $(c)\ \exp(\lambda_3 t)$ and $(d)\ \exp(\lambda_4 t)$.

It is evident that the mean error grows exponentially according to $\lambda_1$ for about 50 days. For such growth, the doubling time of errors is $t_d = (\ln 2)/\lambda_1$.

With $\lambda_1 = 0.03$, the doubling time for small errors is about 2.9 days, comparable to Lorenz's estimate of 2.4 days for the doubling time in the ECMWF model.

When the random error growth starts to deviate from the exponential growth, the magnitude of the mean error is nearly $10^{-2}$, and the subsequent growth rate decreases steadily before reaching saturation. During this phase, the error growth is nonlinear.

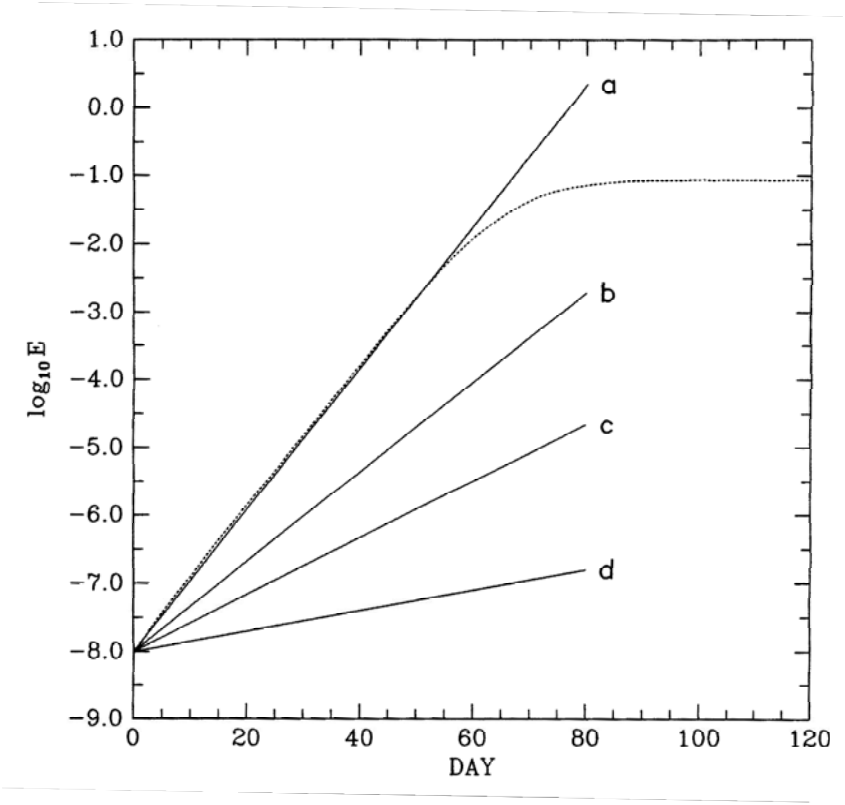

## Growth of errors in chaotic systems

First, small errors grow quasi-exponentially with a certain growth rate during the linear phase of growth. The growth rate is often determined by the largest Lyapunov exponent.

Next, the errors go through a nonlinear phase of growth at a slower growth rate.

Ultimately, the magnitude of the errors approaches or oscillates about a value no larger than the difference between randomly selected states of the system. When the errors reach saturation, the *limit of predictability* has been reached and the predictions become unreliable.

The time taken to reach the limit of predictability depends on the size of the initial error.

## Lorenz's empirical formula for error growth

If $E$ is the mean error, the exponential growth is given by the equation

$$\frac{dE}{dt} = \lambda_1 E$$

The doubling time of the errors is $t_d = (\ln 2)/\lambda_1$.

The errors do not grow forever. The processes limiting the error growth must be represented by nonlinearities in the governing equations which were omitted in the linear tangent equation.

A simple assumption that such nonlinear processes are quadratic in $E$ provides a good approximation. The modified error equation is

$$\frac{dE}{dt} = \lambda_1 E - sE^2$$

where $s$ is so chosen that $E_s = \lambda_1/s$ is the saturation value of $E$.

If $E_0$ is the error at time $t_0$, the error $E$ at a later time $t$ is given by

$$E = \frac{1}{2} E_s \left[ 1 + \tanh\left[ \frac{1}{2} \lambda_1 (t - t_0) - \tanh^{-1}\left( 1 - 2\frac{E_0}{E_s} \right) \right] \right]$$

or

$$\ln\left[ \frac{E\left(1 - E_0 / E_s\right)}{E_0\left(1 - E / E_s\right)} \right] = \lambda_1 \left(t - t_0\right)$$

## Empirical fit to error growth in Lorenz's 28-variable model

The ensemble mean growth of random errors is well approximated by Lorenz's empirical relation with $\lambda_1$=0.03 and $E_s$= 0.086 for the error growth in the 28-variable model.

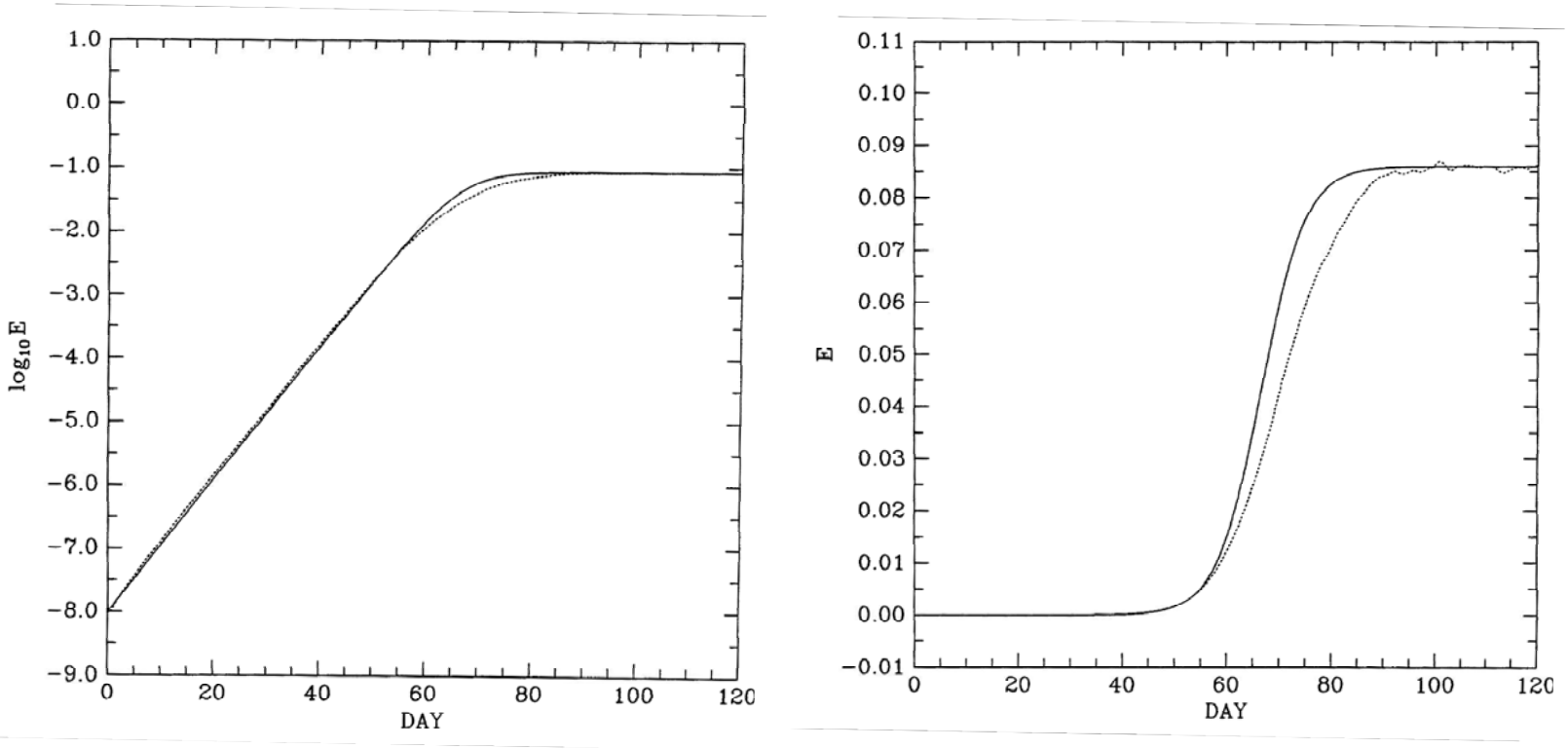

# Predictability in higher dimensional dynamical systems

## Higher dimensional model

The atmospheric system is quite complex, and the general circulation models (GCMs) are too large to be studied as dynamical systems. Here, an idealized spectral model of the atmosphere that includes many scales of motion is studied to understand the nature of the chaotic attractors, their dimensions and predictability. The model is large enough to be studied as a dynamical system with extensive precise computations but not as unmanageable as a GCM.

The model represents a two-layer quasi-geostrophic mid-latitude atmosphere forced by Newtonian heating with dissipation occurring through frictional drags at the surfaces. The model is transformed into spectral form by expanding the dependent variables in a set of orthonormal functions. The spectral truncation determines the smallest scale feature included in the model. The model is studied in a hierarchy of truncation, and the results of four such models, identified as (5X,5Y), (10X,10Y), (15X,15Y) and (20X,20Y), are presented. The (20X,20Y) model, for example, consists of 20 wavenumbers each in zonal (X) and meridional (Y) directions. The number of variables in the model ranges from 110 to 1640.

## Chaos in higher dimensional models

All four models undergo similar sequence of bifurcations for a range of forcing parameter. Smaller scale components, however, shift the bifurcation points as the model becomes more complex. The attractors for lower forcing values are characterized by Hadley and Rossby circulations. Chaotic attractors are obtained after successive Hopf bifurcations.

Time series of temperature in the largest spatial scale

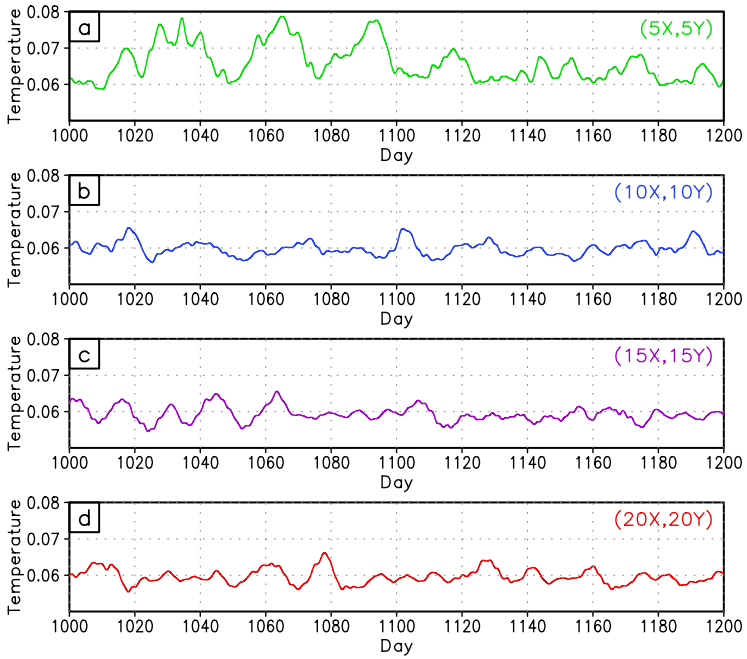


Time series of temperature in the smallest spatial scale

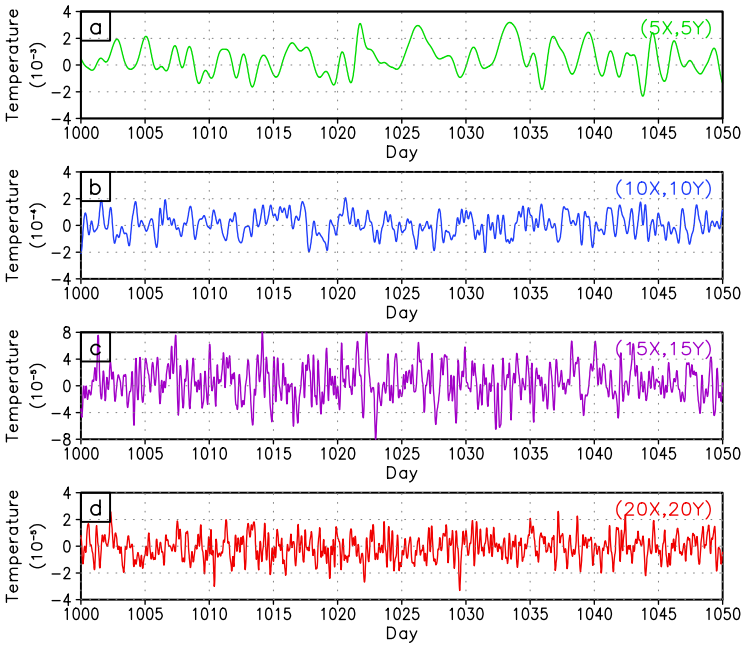

## Dimensions of chaotic attractors in higher dimensional models

It may appear from the time series that the chaotic nature of the attractors has converged, but the degree of chaos, in fact, increases with the order of model truncation. The number of positive Lyapunov exponents and the Lyapunov dimension of the chaotic attractor increase as the model becomes larger (Table). For the (20X,20Y) model, the dimension is more than 368, much larger than the very small values often reported for climate time series.

| Model | Number of Variables | Dimension | Number of Positive Lyapunov Exponents | Largest Lyapunov Exponent |
|---|---|---|---|---|
| 5x,5y | 110 | 35.9 | 14 | 0.043 |
| 10x,10y | 420 | 106.2 | 41 | 0.023 |
| 15x,15y | 930 | 232.2 | 89 | 0.031 |
| 20x,20y | 1640 | 368.4 | 141 | 0.030 |

## Error growth in higher dimensional models

The local evolution of an initial sphere of error into an ellipsoid also shows that number of growing axes increases with the model truncation (Table). The amplification of the longest axis in one day also increases. The local nature of the error growth is seen for all the models in the evolution of an ensemble of initial errors at a particular point in the attractor (Fig. a). The linear growth of errors in the early part of the evolution is described by the amplification of all the axes (both growing and decaying) of the ellipsoid (Fig b).

| Model | Number of growing directions | Longest One-day Amplification | Saturation Value of Error |
|---|---|---|---|
| 5x,5y | 29 | 4.9 | 0.063 |
| 10x,10y | 108 | 10.3 | 0.034 |
| 15x,15y | 247 | 11.8 | 0.035 |
| 20x,20y | 430 | 17.6 | 0.038 |

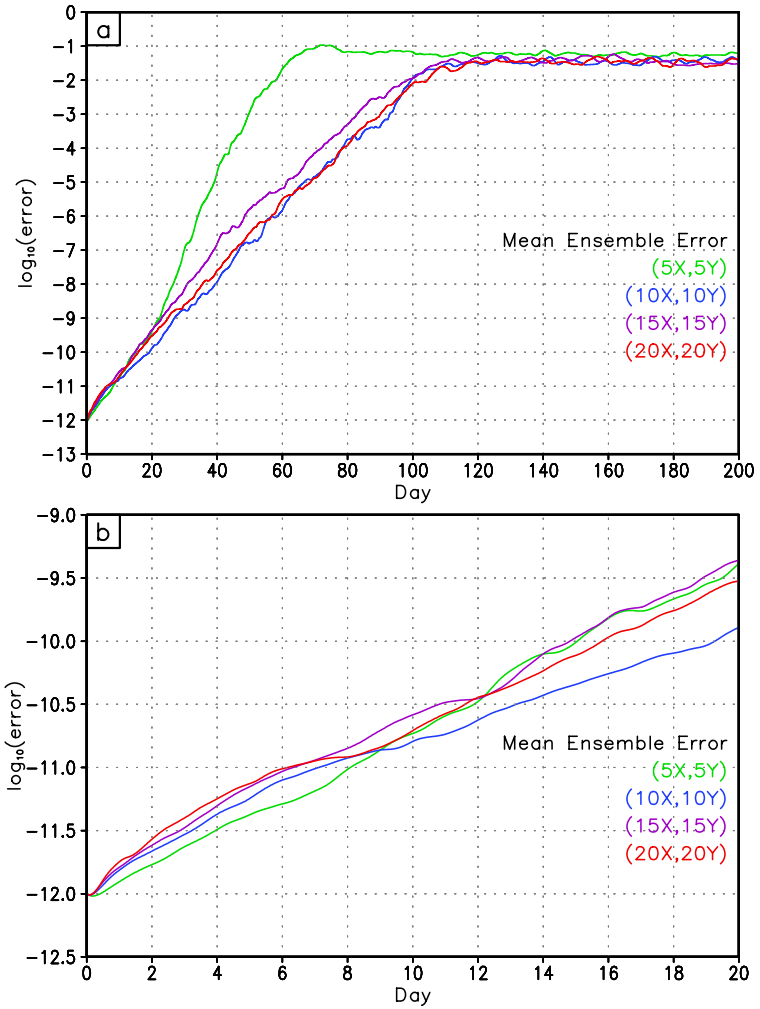

## Error growth in higher dimensional models

The predictability of the models is found by examining the evolution of an ensemble of small initial errors introduced at various points in the attractor (Fig. a). The (5X,5Y) model shows a faster growth rate of errors compared to the other three models. This feature is also reflected in the largest Lyapunov exponent of the models. The limit of predictability is reached in about 80-100 days.

For most part of the linear error growth (except for the initial part), the evolution of the errors can be represented by an empirical formula using the largest Lyapunov exponent only (Fig. b).